Hindawi
International Journal of Energy Research
Volume 2024, Article ID 1105301, 13 pages
https://doi.org/10.1155/2024/1105301

WILEY | Hindawi

Research Article

Enhancing Electric Vehicle Performance with a Hybrid PI-Sliding Mode Controller for Battery Supercapacitor Integration

Monika Suthar,[1] Udaya Bhasker Manthati,[1] C. R. Arunkumar,[1] Punna Srinivas,[1] Faisal Alsaif,[2] and Ievgen Zaitsev[3]

[1]*Department of Electrical Engineering, National Institute of Technology Warangal, Warangal 506004, Telangana, India*
[2]*Department of Electrical Engineering, College of Engineering, King Saud University, Riyadh 11421, Saudi Arabia*
[3]*Department of Theoretical Electrical Engineering and Diagnostics of Electrical Equipment, Institute of Electrodynamics, National Academy of Sciences of Ukraine, Peremogy, 56, Kyiv 57, 03680, Ukraine*

Correspondence should be addressed to Ievgen Zaitsev; zaitsev@i.ua

Received 30 December 2023; Revised 27 March 2024; Accepted 28 March 2024; Published 26 April 2024

Academic Editor: Huaxi Yuan

Nowadays, most of the works are based on electric vehicle usage for sustainable transportation using traditional energy storage device, such as battery. Usage of batteries in electric vehicles is having several disadvantages, for example, life span, temperature, and charge estimation. In this paper, a novel control scheme for battery and supercapacitor- (SC-) based hybrid energy storage system (HESS) using hybrid proportional and integral- (PI-) sliding mode control (SMC) for electric vehicle (EV) applications is introduced and implemented. This HESS with hybrid controller proves the usage of batteries in EVs to its fullest potential. The conventional control strategy for HESS follows two-loop voltage and current PI controllers with low-pass filter (LPF) and involves tuning of multiple control parameters with variations of source and load disturbances. Performance of the system is affected by tuning PI controller constants. A slow response time with linear PI controllers is long which is not advisable for starting and sudden jerk conditions of EVs. Moreover, the PI controller performance is affected by the system parameter variations during load changes. And these parameters are dynamic in nature due to nonideal conditions. In this paper, a hybrid PI-sliding mode controller (SMC) scheme is designed to control the bidirectional DC-DC converters to overcome the drawbacks of aforementioned issues. The combined PI-SMC controller reduces the tuning effort and reduces the effect of shift in operating point in controller performance. Linear modeling is done using small signal analysis for each subsystems. Permanent magnet synchronous machine (PMSM) is used as electric vehicle. The entire system and its controllers are simulated using MATLAB-Simulink, and detailed comparison is carried between conventional PI and proposed hybrid PI-SMC scheme to regulate the DC link voltage. The results are tabulated and show that the hybrid PI-SMC scheme outperforms in transient and steady-state conditions than the traditional PI controller. A scaled hardware prototype of 48 W set-up is developed using dSPACE-1104, and the experimental results have been carried out to verify the proposed system's feasibility.

1. Introduction

It is well acknowledged that rising carbon emissions and limited petroleum availability pose increasing risks to the planet. With almost 28% of global energy use and greenhouse gas emissions coming from the transportation sector [1], the sector has the biggest overall environmental impact. Over 70% of the emissions in this sector come from the road transportation [2, 3]. To reduce the dependency of road vehicles on petroleum supplies and to curb down the emissions, automotive industry is moving towards more sustainable options: hybrid vehicles (being powered by IC engine and electric motor) and fully electric vehicles (EVs) [4]. Recent advancements in power electronics and energy storage systems have aided this trend. Widespread use of EVs is restricted by its energy storage issue. Research is being

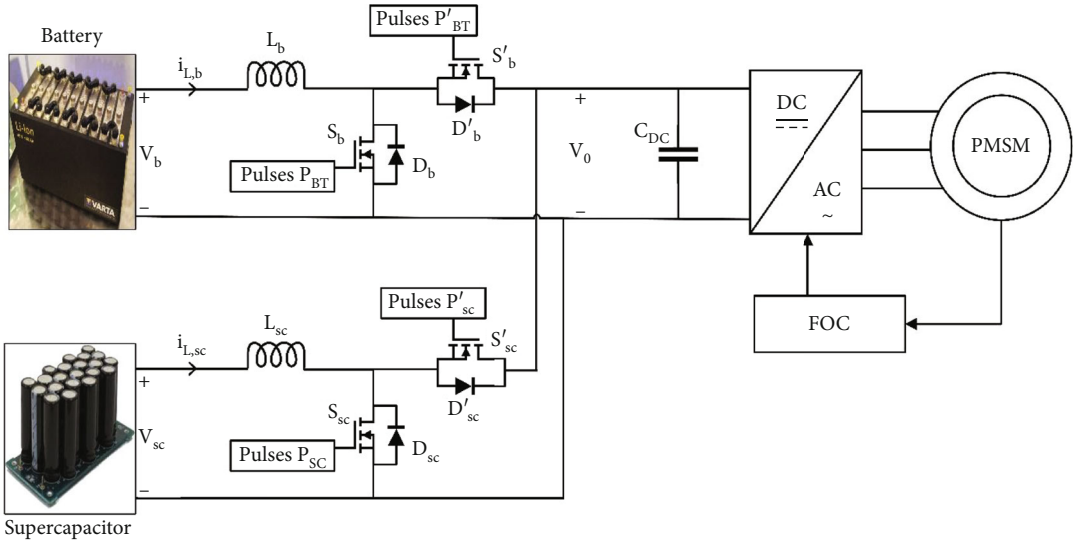

Figure 1: EV electrical system schematic diagram.

carried out to make EVs competitive with IC engine-based vehicles in the market by increasing its electric driving range, improving efficiency, and decreasing its cost [5].

Reliable energy storage source should have (a) high energy density, i.e., capability to deliver energy for long duration, and (b) high power density, i.e., capability to deliver sudden burst of power in with short response time [6, 7]. The available sources like batteries, fuel cells, and SCs do not have both of these characteristics [8, 9]. So there is a need for hybridization of energy sources.

In automotive applications, batteries are the primary energy storage devices. While having a relatively high energy density, they have a relatively low power density, hence characterised by slower dynamics. The lifetime of the battery is degraded if a sudden pulsed current is either supplied by or is injected into the battery, like when the vehicle accelerates or decelerates, respectively [10, 11]. On the other hand, SCs offer high power density, efficiency, and fast dynamics [12]. So using SCs along with battery will provide reliable energy source for EV and also increase battery life span [12–16].

Appropriate energy management strategy should be implemented to effectively use battery-SC combination to reduce stress on battery. Along with this, appropriate control strategy should be used for control of DC-DC converters. Many control strategies have been reported in literature [17]. The most popular controller is linear PI/PID controller due to its easy and simple design and implementation. But due to local linearization in designing the controller, its control performance might degrade as the operating point shifts [18]. To remedy this, several nonlinear controllers are proposed such as fuzzy logic [19], model predictive control [20], and SMC [21, 22].

Model predictive control and SMC methods require complex analysis and high-end computational tools for its implementation, which adds to the cost of vehicle development. As fuzzy logic-based control does not have systematic approach and relies on human knowledge, it needs regular updates in the control system. This paper proposes a hybrid PI-SMC control scheme for HESS. It combines the benefits of simple design of PI control and fast dynamic response of SMC, reducing the design and implementation complexity of the control system compared to the conventional SMC while giving better dynamic performance compared to conventional PI controller. SMC controls the current of the converter giving good dynamic performance of the vehicle, and PI controller controls the bus voltage. Hence, this paper proposes a hybrid controller for the operation of HESS in EV applications. The salient features of the proposed scheme are as follows:

(1) Detailed modeling of energy sources, bidirectional DC-DC converter, permanent magnet synchronous motor, and their controllers is shown

(2) A hybrid PI-SMC cascaded control scheme employing SMC for inner current loop, and PI controller for HESS outer voltage control is presented for DC bus voltage regulation

(3) The performance analysis of the battery-SC system for inverter-motor load considering two modes of operation, motoring mode and regenerative mode, is presented using MATLAB-Simulink software

(4) A comparative performance analysis between traditional PI controller and hybrid PI-SMC controller is presented for regulating DC bus voltage under varying speed and torque conditions of motor load

The remaining paper has been organized as follows: Details of system components, modeling, and system interfacing are discussed in Section 2. Design of proposed controller for bidirectional DC-DC converter and motor controller is discussed in Section 3. Simulation results are discussed in Section 4. Experimental work and results are presented in Section 5. And conclusion of the work is presented in Section 6. At the end, more relevant references are included.

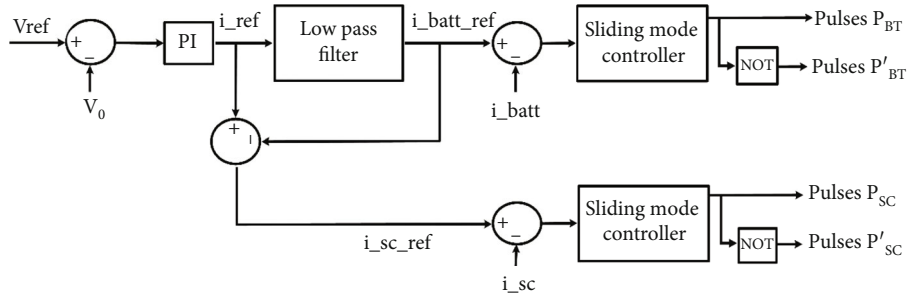

Figure 2: Closed-loop control scheme of HESS.

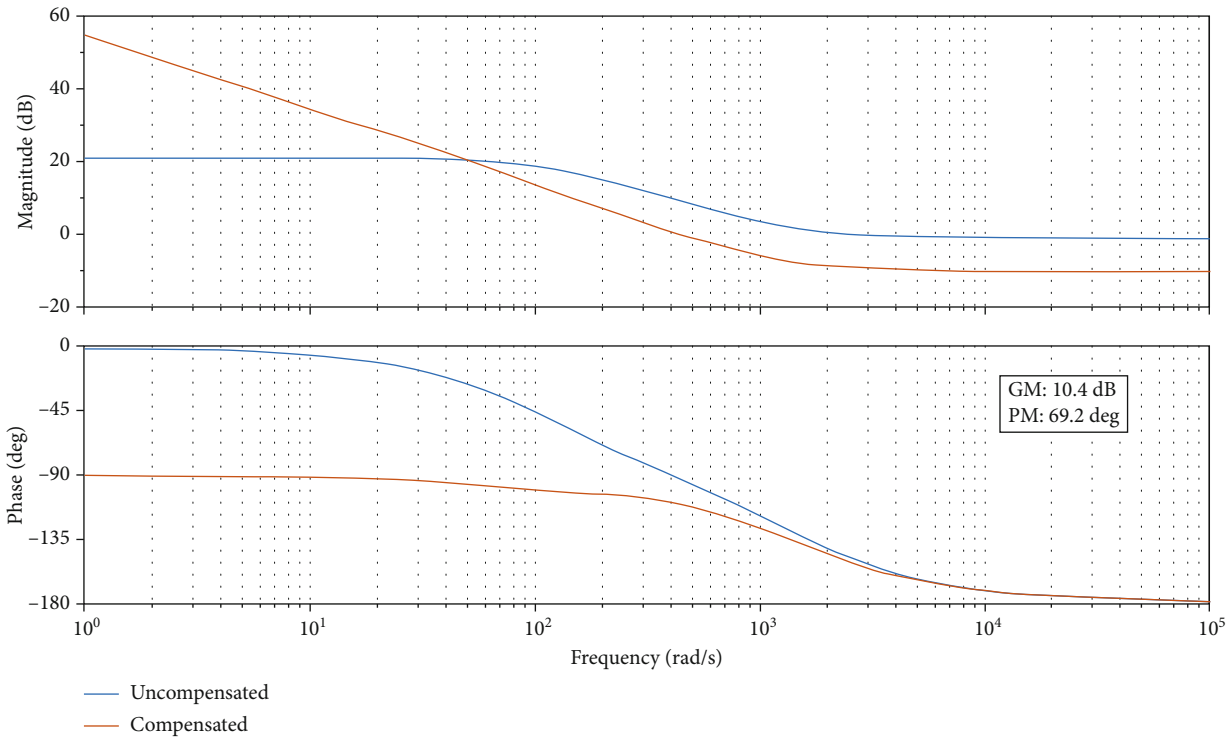

Figure 3: Bode diagram of open loop transfer function of the outer voltage loop with PI controller.

2. System Configuration and Modeling

The drive train system of EV consists of battery-SC-based hybrid energy storage system, bidirectional buck-boost converters, and PMSM drive. Source is connected in active parallel topology, where each source is connected to a bidirectional converter and the converters are connected in parallel to a common DC link. The advantage of this topology is that it provides separate control over the battery and SC current. The control of bidirectional converters to maintain stable DC link voltage is done using SMC. DC link is further connected to a three-phase inverter and PMSM drive as load. Control of PMSM is done through field oriented control (FOC) algorithm. The schematic of the system is given in Figure 1.

Battery and SCs are the two sources of the system, which are connected in parallel to share the load current in variation with the speed of the PMSM. The detailed modeling and operation are explained in the following sections. The energy exchange among the storage devices is an important aspect, which is demonstrated both simulation and hardware results. Development of bidirectional converters and inverters and power semiconductor devices is used. Ideal characteristics of power semiconductor devices are considered for simulation work.

2.1. Bidirectional DC-DC Converter. It allows energy flow in both directions: from source to load (during discharging mode) and from load to source (during charging mode). The bidirectional converter used is a synchronous boost/buck converter, which replaces diode with semiconductor switch to enable power flow in reverse direction from load to source.

When power flow is from source to load, converter operates in boost mode with devices (S_b, D_b') and (S_{sc}, D_{sc}') active in respective converters. When power flow i_d from load to

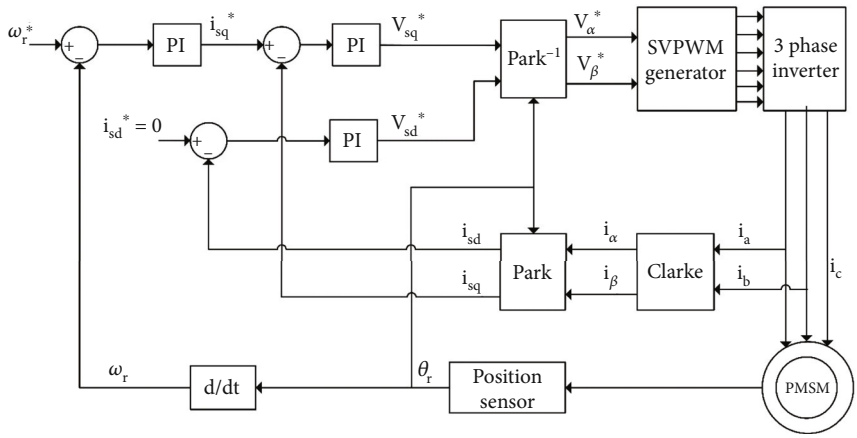

Figure 4: FOC algorithm for control of PMSM.

source, converter operates in buck mode with devices (S_b', D_b) and (S_{sc}', D_{sc}) active. DC bus voltage (V_{DC}) is maintained at a constant reference value by regulating the charging and discharging of the capacitor.

The mathematical model of the bidirectional DC-DC converter can be written as

$$\frac{di_L}{dt} = \frac{V_{dc}}{L} - (1-u)\frac{v_o}{L},$$
$$\frac{dv_o}{dt} = \frac{i_L}{C}(1-u) - \frac{v_o}{RC}, \tag{1}$$

where u is the state of switch.

$$u = \begin{cases} 0, S_b(\text{or})S_{sc}\text{is Off}, \\ 1, S_b(\text{or})S_{sc}\text{is On}, \end{cases} \tag{2}$$

where i_L is the inductor current (A) ($i_{L,b}$, $i_{L,sc}$), V_{DC} is the DC source voltage (V) (V_b, V_{sc}), V_o is the output voltage/DC link voltage (V), L is the inductance (H), C is the capacitance (F), and R is the load resistance (Ω).

2.2. PMSM Modeling. PMSM are increasingly being used in EV due to their simple construction, high efficiency, and high power density. There are two types of PMSM motors: surface-mounted PM and interior PMSM. In this paper, surface-mounted PMSM is used. Its mathematical model can be described by following equations [23].

2.2.1. Electrical System.

$$\frac{d}{dt}i_{ds} = \frac{1}{L_s}v_d - \frac{R}{L_s}i_{ds} + P\omega_m i_{qs},$$
$$\frac{d}{dt}i_{qs} = \frac{1}{L_s}v_q - \frac{R}{L_s}i_{qs} - P\omega_m i_{ds} - \frac{\lambda P\omega_m}{L_s}, \tag{3}$$
$$T_e = 1.5P\,\lambda i_{qs}.$$

Table 1: Parameters of system used for simulation.

S. no.	Parameter	Value
Source: bidirectional converter		
1	Battery	150 V, 14 Ah
2	Supercapacitor	150 V, 16 F
3	Output DC link voltage	300 V
4	Bidirectional converter inductor	8 mH
5	DC link capacitor	400 μF
Load component: motor		
6	Stator resistance	0.129 Ω
7	Armature inductance (Ld, Lq)	1.53 mH
8	Flux linkage	0.1821 V·s
9	Pole pairs	4
10	Inertia	0.053 kgm^2

Here, i_{ds} is the d-axis stator currents (A), i_{qs} is the q-axis stator current (A), V_{ds} is the d-axis stator voltage (V), V_{qs} is the q-axis stator voltage (V), λ is the flux produced by permanent magnets (Wb), L_s is the stator inductance (H), R is the stator winding resistance (Ω), ω_m is the mechanical speed of rotor (rad/s), P is the number of pole pairs, and Te is the electromagnetic torque (N-m).

2.2.2. Mechanical System.

$$\frac{d}{dt}\omega_r = \left(\frac{1}{J}T_e - F\omega_r - T_L\right),$$
$$\frac{d}{dt}\theta_r = \omega_r, \tag{4}$$

where J is the rotor inertia (kg·m^2), F is the viscous friction (N·m·s), and θ_r is the mechanical rotor angle (rad).

3. Control System Design

3.1. Bidirectional Converter Control. Control of bidirectional converters is done using a cascaded control strategy as

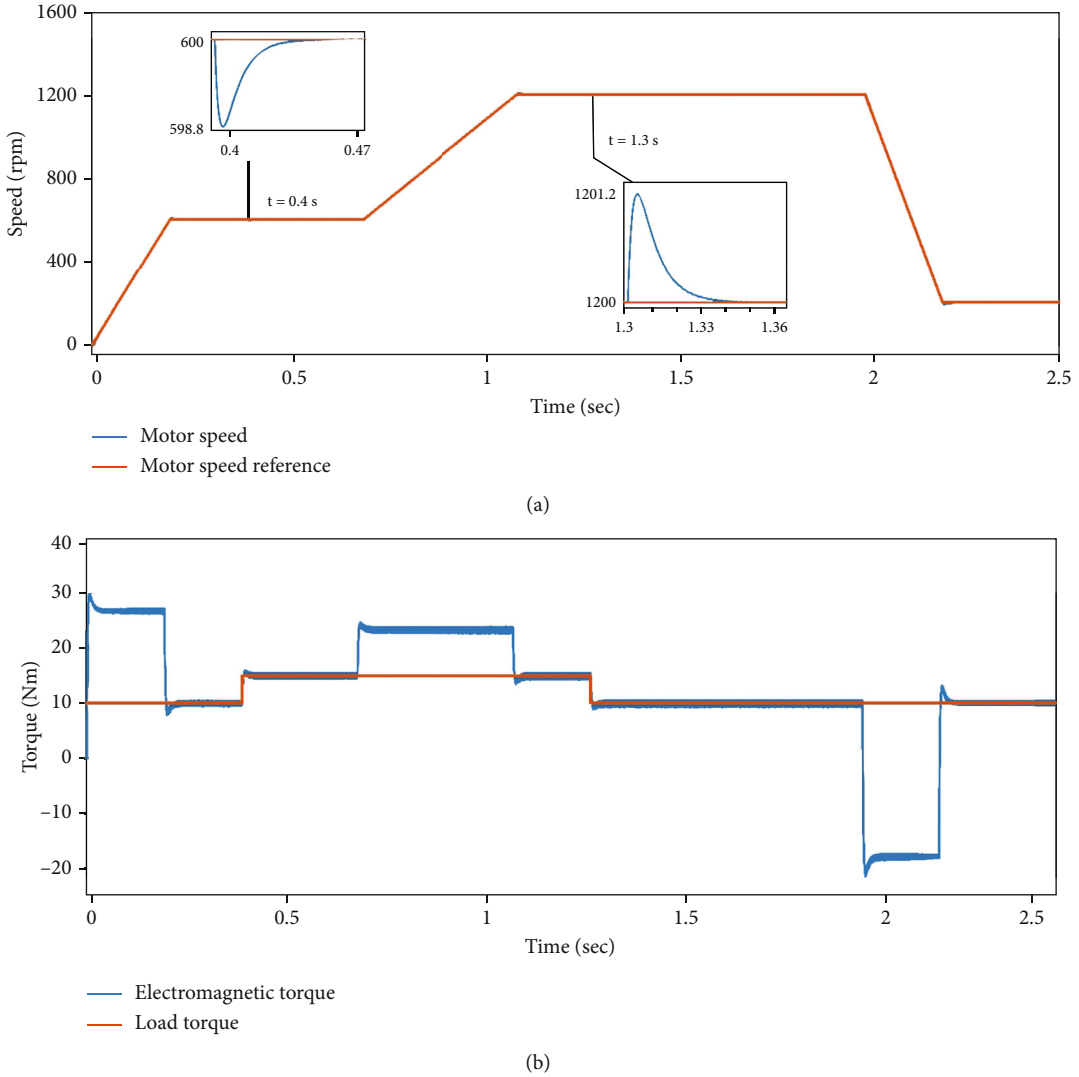

Figure 5: (a) Reference and actual speed of motor. (b) Electromagnetic torque and load torque of motor.

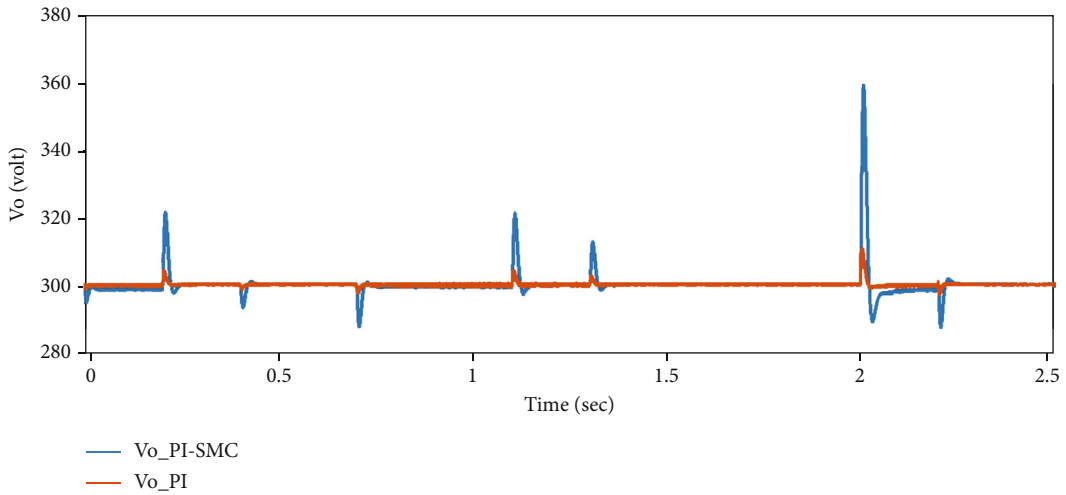

Figure 6: DC link voltage waveform of PI-SMC and PI-based control.

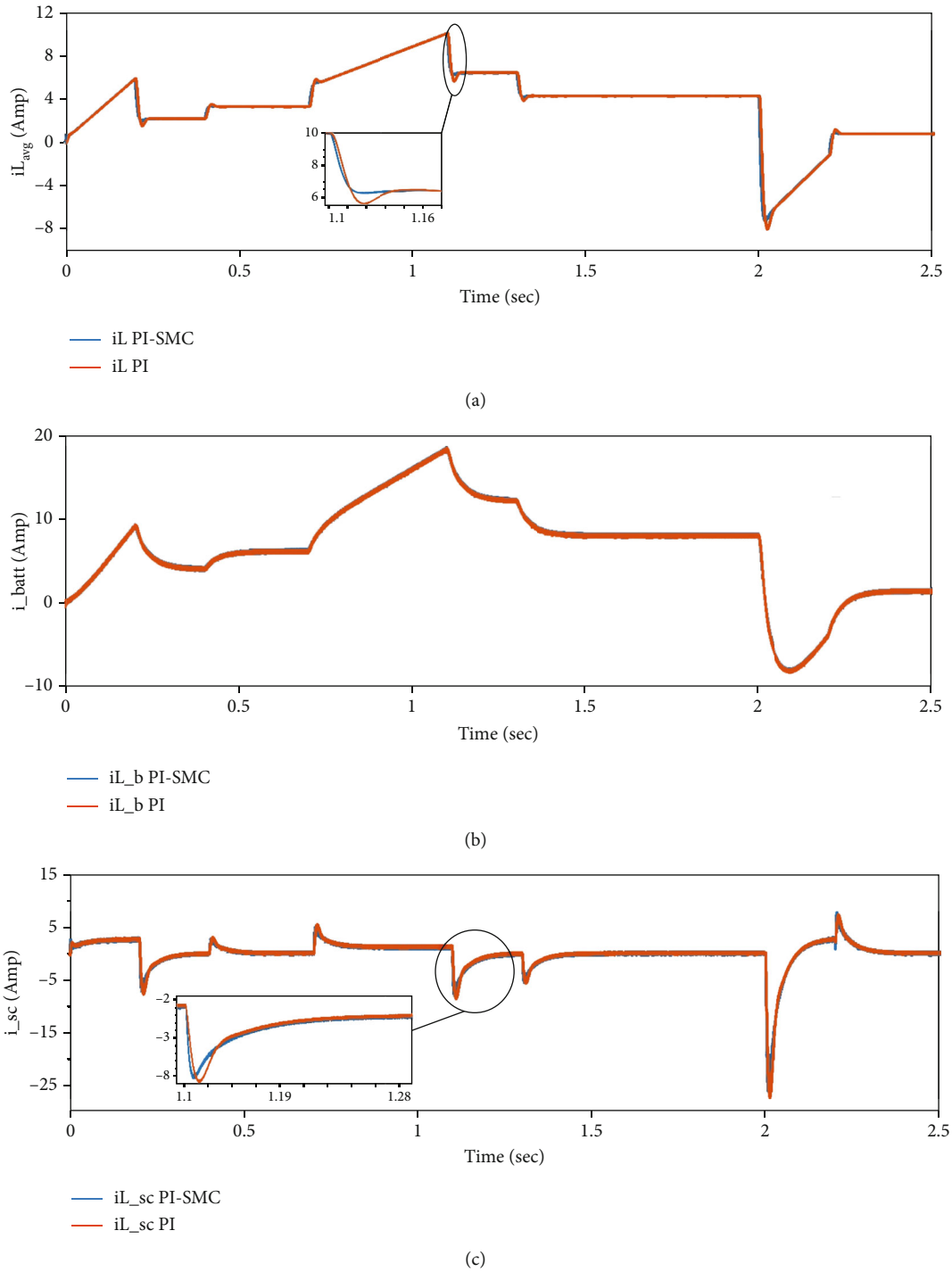

Figure 7: HESS current: (a) load current; (b) battery current; (c) supercapacitor current of PI-SMC and PI-based control.

shown in Figure 2. Outer loop for DC link voltage regulation employs PI controller to generate overall current reference. This current reference is then split in two parts: battery current reference, which is low-frequency component, and SC current reference which is high-frequency component. Battery current reference is generated by passing total current reference through a low-pass filter. SC current reference is generated by subtracting battery reference from total current reference. Inner current loop uses sliding mode control (SMC) to track the reference currents. The low-pass filter cutoff frequency is selected as 30 rad/sec [18].

3.1.1. Outer Voltage Loop: PI Controller. For controller tuning purpose, open loop output voltage to inductor current

Table 2: Comparison of DC link voltage disturbance for PI-SMC and PI-based control.

S. no.	Time (in sec)	Voltage undershoot/overshoot (in volts)	
		PI-SMC	PI
1	0.2	4.1	21.69
2	0.4	1.26	6.83
3	0.7	2.48	12.6
4	1.1	3.8	21.26
5	1.3	2.43	12.74
6	2	10.5	59.29
7	2.2	2.41	12.89

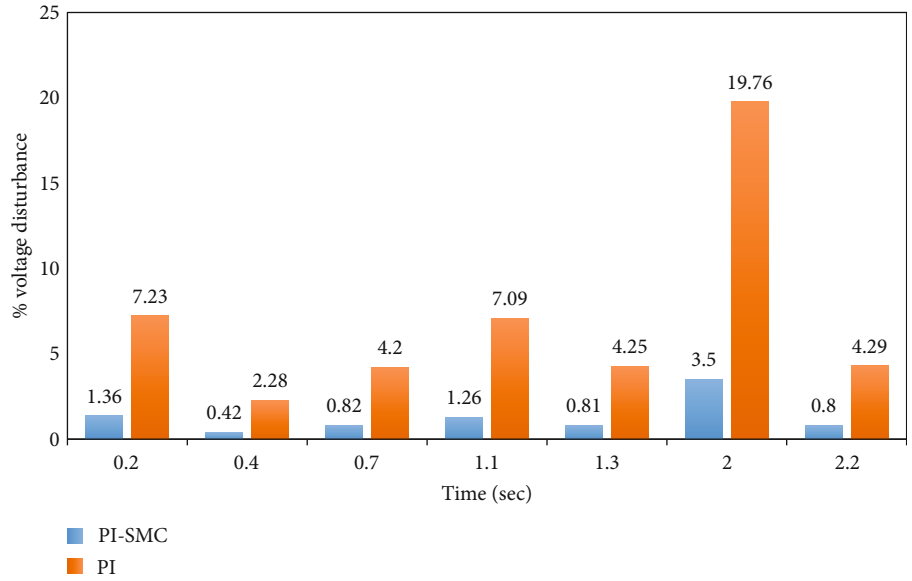

Figure 8: Percentage (%) DC link voltage disturbance in for PI-SMC and PI controllers.

transfer function of boost converter is obtained using small signal modeling as follows [24, 25]:

$$\frac{\hat{v}}{\hat{i}_L} = \frac{-0.016s + 22.5}{0.018s + 2}. \quad (5)$$

Transfer function of PI controller with K_p (0.34) and K_i (46.37) is obtained as

$$\mathrm{TF}_{\mathrm{PI}} = \frac{0.34s + 46.37}{s}. \quad (6)$$

Figure 3 shows bode diagram of uncompensated and compensated system. Controller is designed to have satisfactory gain and phase margin for stable performance of converter. Bandwidth of loop is kept 450 rad/s to obtain good phase margin considering the presence of right half plane zero at 1406.05 rad/s. Phase margin of 69.2° is obtained with gain margin of 10.4 dB.

3.1.2. Inner Current Control Loop: SMC. The switched converters are nonlinear because of the discrete switches that changes the dynamics of their systems when changing state. This class of system is known as variable structure systems (VSS). SMC is a control technique specialized for VSS [26, 27]. SMC has many benefits such as robustness, stability under large supply and load variations, good dynamic performance, and ease of implementation.

(1) Designing SMC. SMC makes the system variable to stay on a fixed path in state space which is called the sliding surface. There are three conditions which must hold in order for the system to converge.

(a) Existence Condition. States of the subsystem are directed in the direction of the sliding surface

$$\lim_{\sigma \longrightarrow 0} \frac{d\sigma}{dt} < 0. \quad (7)$$

(b) Hitting Condition. Initial state condition should lead system towards the sliding surface

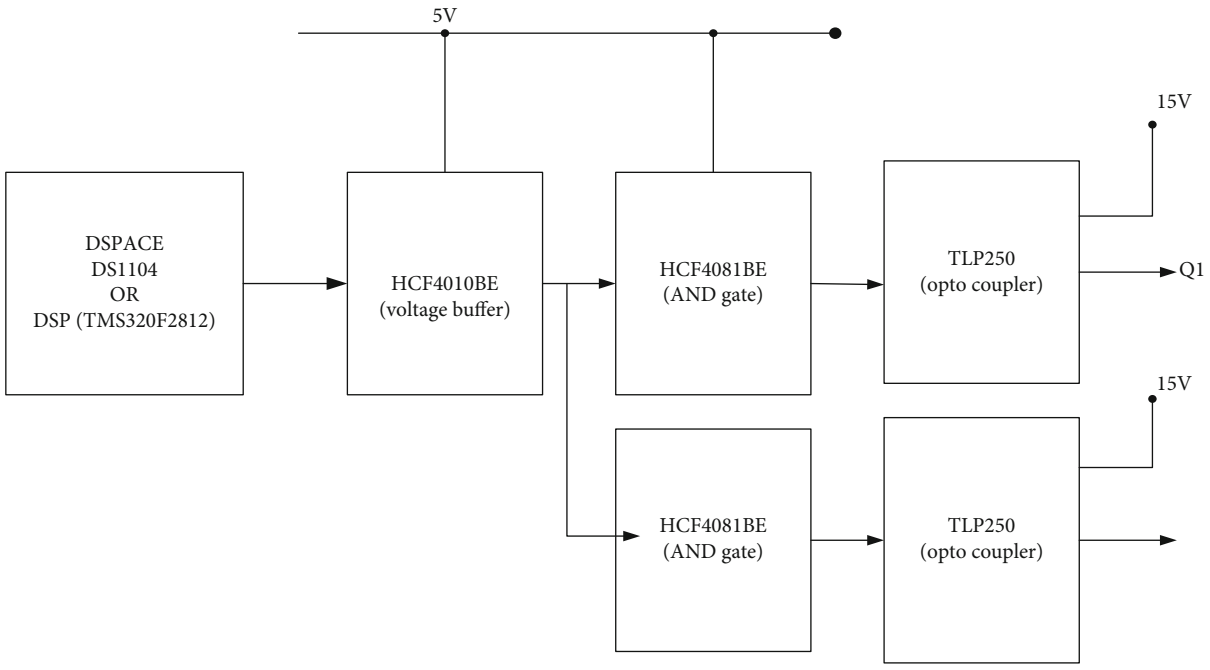

(a)

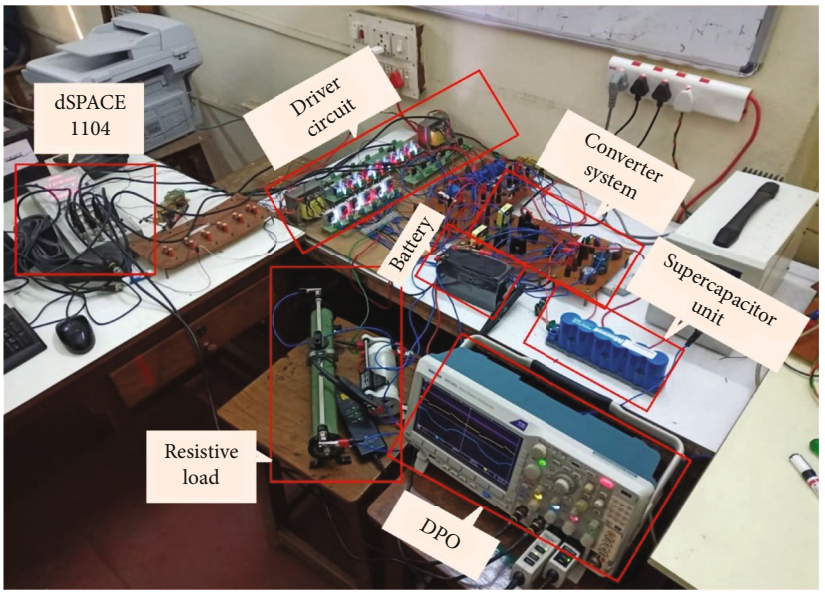

(b)

Figure 9: (a) Gate driver circuit using A3120 optocoupler. (b) Hardware setup of prototype system.

$$[x_i^+] \in \sigma(x) < 0,$$
$$[x_i^-] \in \sigma(x) > 0. \tag{8}$$

(c) Stability Condition. The movement along the sliding surface should be directed towards a stable point

$$u = \begin{cases} u^+ \text{ for } \sigma(x) > 0, \\ u^- \text{ for } \sigma(x) < 0. \end{cases} \tag{9}$$

Here, SMC is used to control the inductor current. Considering inductor current error as state variable,

$$x_1 = i_L,$$
$$e = i_L - i_{\text{Lref}},$$
$$i_{\text{Lref}} = (v_o - V_{\text{oref}})\left(\frac{K_p + K_i}{s}\right). \tag{10}$$

The sliding surface is defined as

$$\sigma(e) = \lambda e + \dot{e} = 0. \tag{11}$$

The SMC determines control action u. A hysteresis window is designed allowing a small error. The control action is chosen as

$$u = \begin{cases} 1 & \text{for } \sigma(e) < -k, \\ 0 & \text{for } \sigma(e) > k, \\ \text{previous state} & \text{for } -k < \sigma(e) < k. \end{cases} \quad (12)$$

3.2. Field Oriented Control of PMSM. Figure 4 shows the block diagram representation of the FOC algorithm of PMSM. In this work, CLARK and PARK transformation techniques are used to do the conversion from 3-phase to 2-phase system and incorporate speed control. Different types of sensors are used to sense speed, position, voltage, and current signals at different levels. The rotor position θ_r is sensed using a position sensor. This angle is then converted to electrical angle and is then used in the Park transformation. The motor current is sensed from any two phase and then is converted into direct component i_{sd} and quadrature component i_{sq}. Derivative of the rotor angle gives rotor speed ω_r. This speed is compared with speed reference ω_r^*, and the error is given to the PI controller. Output of this speed controller gives reference quadrature/torque component of current i_{sq}^*. Flux/direct component of current reference i_{sd}^* is zero for PMSM as flux is generated by permanent magnets and stator current does not require to produce any additional current [28].

Current i_{sd} and i_{sq} are compared with their reference value, and the errors are given to PI controllers. The outputs of these current controllers are reference voltages V_{sd}^* and V_{sq}^* which are converted to V_α^* and V_β^* using inverse Park transformation and are given to space vector PWM (SVPWM) algorithm module to generate inverter gating signals [28]. SVPWM is popular among the other modulation techniques for better usage of DC source.

4. Results and Discussions

4.1. Simulation Work. System model and control scheme were simulated using MATLAB-Simulink software. The parameters used in simulation are as shown in Table 1. Motor speed (N) and torque (τ) waveforms are shown in Figures 5(a) and 5(b), respectively. Electric vehicle undergoes various modes such as starting, acceleration, constant speed, deceleration, and braking phases at various time intervals. It is due to starting, accelerating, free running, decelerating, and braking requirements from zero speed to rated speed and vice versa. An EV follows speed-time reference curve under closed-loop operation with minor fluctuations with respect to load variations as shown Figures 6 and 7.

Average load current, battery current, and SC current waveforms are shown in Figure 7. Certain percentage of load current is shared by battery and SCs during transient conditions. Battery current is controlled to change slowly and provide steady-state component, and SC current provides the transient component. Figure 6 shows a bar chart comparison

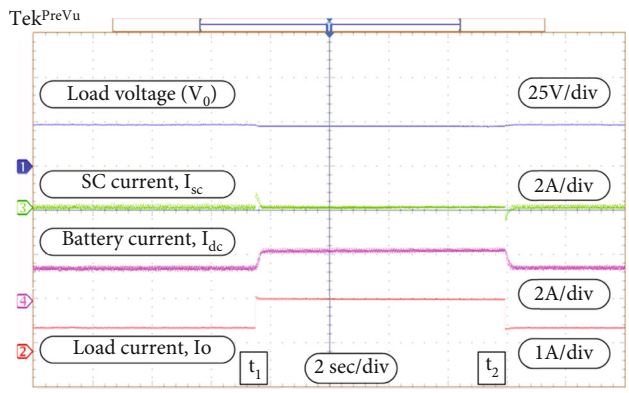

Figure 10: Experimental results with PI controller.

of DC link voltage regulation performance of PI-SMC and PI control under various disturbance conditions.

4.2. During Accelerating Period of the Motor. At starting condition, $t = 0$ sec to 0.2 sec motor is accelerated to speed of 600 RPM. Motor is again accelerated from 0.7 sec to 1.1 sec to increase speed to 1200 RPM. It can be observed from Figure 5(b) that during acceleration period, electromagnetic torque by motor is more than the load torque.

At the start of accelerating period (0 sec, 0.7 sec), there is sudden increase in electromagnetic torque of motor and hence increase in load current demand from HESS as shown in Figure 5(a). During these transients, battery current varies smoothly over the period of time and SC supplies the transient component of load current by supplying the excessive power. During acceleration period, motor power demand slowly increases till it reaches to a rated speed. At the end of acceleration period (0.2 sec, 1.1 sec), when speed reference becomes constant, there is sudden dip in power demand from HESS. This can be seen by average load current waveform in Figure 7(a). The battery current varies smoothly over the period of time, and SC supplies the transient component of load current by absorbing the excessive power. So this bidirectional DC-DC converter operates in buck mode and charges the SCs.

Due to this sudden increase/decrease in load current, DC link voltage undershoots/overshoots as shown in Figure 6. The magnitude of undershoot/overshoot is much less in case of PI-SMC than in case of PI controller. Also, it is observed that the voltage waveform settles faster in case of PI-SMC. These are the required conditions to enhance the performance of a battery and lowering the overshoots during starting. Similarly, to reduce the undershoots during minimum speed conditions in electric vehicles.

4.3. During Constant Speed of the Motor. At $t = 0.2$ sec to 0.7 sec, 1.1 sec to 2 sec, and from 2.2 sec to 2.5 sec, motor is given constant speed reference of 600 RPM, 1200 RPM, and 200 RPM, respectively. At 0.4 sec, load torque on vehicle is changed from 10 N-m to 15 N-m. It can be observed from Figure 5(a) that vehicle follows speed reference with minor fluctuations. At $t = 1.3$ sec, load torque on vehicle is again

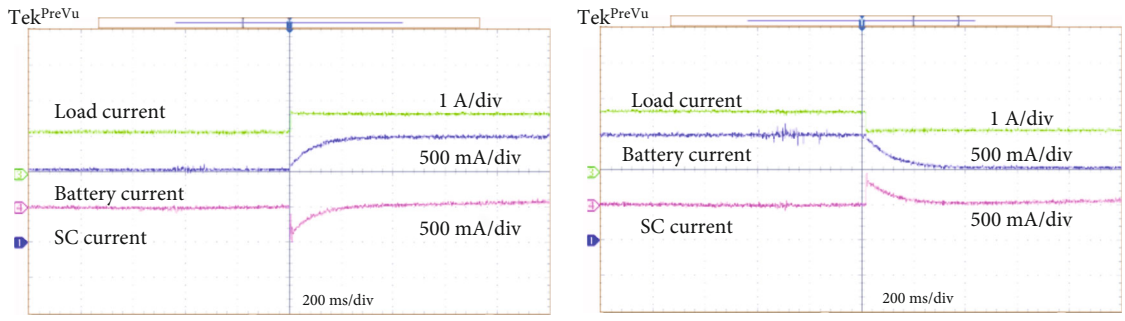

Figure 11: Experimental results for variation in load, battery, and SC currents during (a) load increment and (b) load decrement.

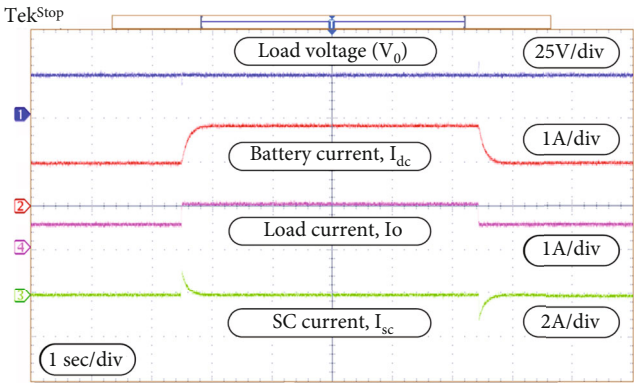

Figure 12: Experimental results with PI-SMC controller.

changed from 15 N-m to 10 N-m. Again, vehicle follows the speed reference satisfactorily.

As the electromagnetic torque follows load torque, power demand from HESS at 0.4 sec increases. This leads to sudden increase in load current, which is divided into battery and SC current components. Both battery and SCs get discharged during this period. At $t = 2$ sec, again electromagnetic torque changes, leading to decrease in load power demand. To provide transient component, SC current becomes negative, charging SCs. Observe voltage undershoot at 0.4 sec and overshoot at 1.3 sec due to these disturbances. As previously observed, hybrid controller gives better dynamic performance compared to PI controller.

4.4. During Deceleration Period of the Motor. At $t = 2$ sec to 2.2 sec, motor is decelerated and speed decreases from 1200 RPM to 200 RPM. During this period, electromagnetic torque becomes less than load torque. It is observed from Figure 5(b) that electromagnetic torque becomes negative and motor drive is operating in regenerative region. Power is fed back into HESS to charge battery and SC by operating the bidirectional DC converter in buck operation.

During deceleration, load current becomes negative. This current is divided into battery and in SC current, where SC provides the transient component. Here, both battery and SC current become negative, hence charging of both battery and SCs and both the DC converter operates in buck mode. Due to change in load current, there is overshoot in DC link voltage as shown in Figure 6. As previously observed, hybrid controller gives better dynamic performance compared to PI controller. Table 2 shows the comparative results of overshoot/undershoot of DC link voltage at different disturbances.

It can be seen that voltage regulation performance in PI-SMC scheme is superior compared to PI control. Also, the settling time with SMC is less than PI control. Settling time using SMC scheme is 15-20 msec, while in case of PI, it is 55-60 msec.

At $t = 2$ sec, voltage overshoot in PI-SMC regulated system is 10.5 V (3.5%), while in PI regulated system, it is 59.29 V (19.76%). The voltage is much better regulated using PI-SMC which allows us to use smaller value of DC link capacitor for the same desired voltage regulation performance. Figure 8 shows the comparison of % voltage disturbance produced at different instants.

5. Experimental Results

A hardware prototype is developed to test the proposed PI-SMC control scheme for battery-SC system as shown in Figure 9(b). A 12 V and 7 Ah lead-acid battery and 16 V and 58F Maxwell Technologies BMOD0058 SCs are used. Experiments are done for 48 W output consisting of resistive load. Two of 25 Ω resistors connected in parallel, and a control switch is used to emulate load disturbance. Closed-loop control is implemented using dSPACE-1104 controller. Two boost converters are used to connect the battery and SC to the DC link, and additional gate drivers are used to drive the IRFP460 MOSFETs. Initially, the EV system is controlled by PI controller and tested with different load disturbances to analyze the performance. Later, same system is analyzed with PI-SMC controller and compared the performances.

For generating gate signals from the digital signals of DS1104, peripheral circuits are needed. Mainly two boards are required: (i) gate driver circuit and (ii) power supply for gate driver. The functions performed by the boards are as follows:

(1) Generating gating signals to control the power semiconductor devices

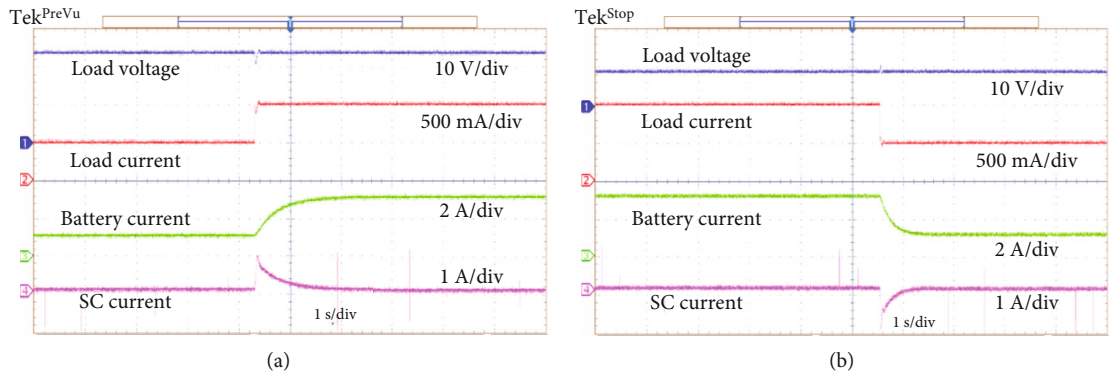

Figure 13: Experimental results for variation in load voltage, battery, and SC currents during (a) load increment and (b) load decrement.

(2) Providing isolation between control circuit and power circuit

(3) Providing power supply to ICs used in control circuit

The gate driver circuit provides isolation between the control and power circuits is shown in Figure 9(a). Every MOSFET (IRFP460N) of power circuit has its own gate drive circuit consisting of isolated DC supply, delay unit. The signal is then fed to optocoupler A3120 which provides electrical isolation for each power semiconductor switch. The digital signals generated by dSPACE-1104 are given to HCF4010BE buffer. The buffer output is connected to HCF40810BE via RC to remove slew rate. The TURN-ON delay provided between top and bottom switches is 1 msec using an RC and fast recovery diode (FR107). The output of HCF40810BE is given to optocoupler (A3120), which provides isolation and generates required gate signal to drive the MOSFET. The bottom switches of two-level inverter have common source, so only one source is enough for optocoupler.

5.1. PI Controller. Figure 10 shows results of system controlled using PI controller. Initially load current is 0.5 A which is supplied by battery alone. At $t = t_1$, there is a step change in load demand results in increase in load current from 0.5 A to 1 A. Transient component of current is supplied by SCs, while the battery current changes slowly to reach steady-state load current value. SC current is positive, as it is being discharged. Load voltage is regulated with a small error. At $t = t_2$, there is a step change in load current from 1 A to 0.5 A. SCs absorb the excessive power and charging itself. Hence, SC current is negative. In Figure 11, the enhanced view of load increment and decrement is depicted. In Figure 11(a), the load increases from 1 A to 1.5 A and the battery supplies additional current required. Also, the supercapcitor discharges the additional transient power required. Similarly, in Figure 11(b), the load current reduces to 1 A to 0.5 A and SC absorbs the additional current.

5.2. PI-SMC Controller. Figure 12 shows results of proposed system controller using PI-SMC controller. At $t = t_1$, the load demand changes from 0.5 A to 1 A and battery current increases to 2 A. The battery discharge rate is controlled so that the battery provides only low-frequency current. SCs provide transient component of the current. Similarly, at $t = t_2$, there is a step change in load current from 1 A to 0.5 A. It is observed that DC bus voltage is regulated during disturbances with minute errors while in case of PI controller, a small error is observed. Further, the SCs take more transient current and settle the DC grid voltage rapidly compared to traditional PI controller.

In Figure 13, the experimental results with PI-SMC controller are presented during load increment and decrement. In Figure 13(a), the load increased from 500 mA to 1 A and battery current is increased to support the load requirement. The SC current supplies the sudden transient requirement and DC bus stabilized with less oscillation. In Figure 13(b), the load disturbance is reduce from 1 A to 500 mA, and battery and SC together mitigate the sudden change in load and DC bus voltage maintained at 24 V.

Results with the PI controller showed that during load changes, the battery and SC played complementary roles. The battery supplied slow, low-frequency current, while the SC provided rapid transient support, regulating the load voltage with minor errors. The enhanced view of load changes revealed the dynamic response of the system. In contrast, the PI-SMC controller demonstrated superior performance, maintaining DC bus voltage stability during load disturbances with minimal errors and quicker recovery compared to the traditional PI controller. Experimental results validated the effectiveness of the PI-SMC control strategy in regulating the battery-SC system under varying load conditions.

6. Conclusion

The results are based on laboratory simulation and experimentation work. Battery life span mentioned by the companies is not the same as what the user getting. This research work is vital and still hardware experimentation with motor to be developed. This novel concept is to be incorporated in EVs to enhance better life during transient state. Settling time and percent of overshoot/undershoot are reduced using the proposed control method. Due to high cost of SCs, the use of SCs in EVs is not seen.

The proposed control strategy using hybrid PI-SMC is designed to control a HESS comprising battery and SC as sources. The SMC is a nonlinear, robust control technique combined with a simple PI controller to achieve better DC link voltage regulation, less system parameter dependency, and easy controller tuning. Considering PMSM as load, the system is simulated to check performance under varying driveline speed and torque conditions. During the power transients, the proposed scheme allows the battery current to change slowly and provides a low-frequency component of load current. At the same time, SC reacts quickly to provide high-frequency components. This reduces losses and thermal stress on the battery and prevents overshoot of battery current, improving battery health and life. The comparative study of the proposed PI-SMC and conventional PI controller shows that employing PI-SMC and DC link voltage is better regulated than a PI controller, thus reducing DC link capacitor value. The proposed hybrid controller also gives a faster response with reduced settling time. This work is developed for promoting EVs with HESS, which directly reduces environmental pollution, global warming, and CO, and these are integral parts of sustainability in this modern world. The scope of this research can be expanded to encompass fixed sliding mode control, ensuring constant switching frequency operation. Additionally, there is room for further development in the form of an energy management strategy aimed at effectively controlling the operation of the HESS.

Nomenclature

Q: Charge in coulomb
I_{sc}: Supercapacitor current in amperes
V_{sc}: Supercapacitor voltage in volts
V_b: Battery voltage in volts
i_b: Battery current in amperes
V_o: Output voltage in volts
C_{DC}: DC link capacitor in farads
$i_{DC-link}$: DC link current in amperes
τ_e: Electromagnetic torque in N-m
τ_L: Load torque in N-m
V_{ref}: Reference voltage in volts
I_{ref}: Reference current in amperes
ω_r: Rotor speed in RPM
$\omega_r{}^*$: Rotor reference speed in RPM
k_p: Proportional constant
k_i: Integral constant
t: Time in seconds
Θ_r: Mechanical rotor angle in radians
L: Inductor in henry
F: Frequency in Hz.

Abbreviations

DC: Direct current
MOSFET: Metal oxide semiconductor field effect transistor
HESS: Hybrid energy storage systems
PI controller: Proportional and integral controller
TF: Transfer function
LPF: Low-pass filter
GM: Gain margin
PM: Phase margin
SMC: Sliding mode controller
PMSM: Permanent magnet synchronous machine
EV: Electric vehicle
IC Engine: Internal combustion engine
SCs: Supercapacitors
SOC: State of charge
FOC: Field oriented control
RPM: Rotations per minute.

Data Availability

Data is available on request.

Additional Points

Future Scope. An extension of work can be done using three different sources such as PV, battery, SCs, and energy exchange among themselves using PI-SMC and also incorporated with actual PMSM and its speed control.

Conflicts of Interest

The authors declare that they have no conflicts of interest.

Acknowledgments

This work was supported by the Researchers Supporting Project number (RSPD2024R646), King Saud University, Riyadh, Saudi Arabia.

References

[1] B. V. Ayodele and S. I. Mustapa, "Life cycle cost assessment of electric vehicles: a review and bibliometric analysis," *Sustainability*, vol. 12, no. 6, p. 2387, 2020.

[2] H. T. Pao and C. C. Chen, "Decoupling strategies: CO_2 emissions, energy resources, and economic growth in the Group of Twenty," *Journal of Cleaner Production*, vol. 206, pp. 907–919, 2019.

[3] M. Rapa, L. Gobbi, and R. Ruggieri, "Environmental and economic sustainability of electric vehicles: life cycle assessment and life cycle costing evaluation of electricity sources," *Energies*, vol. 13, no. 23, p. 6292, 2020.

[4] M. K. Hasan, M. Mahmud, A. A. Habib, S. M. Motakabber, and S. Islam, "Review of electric vehicle energy storage and management system: Standards, issues, and challenges," *Journal of Energy Storage*, vol. 41, article 102940, 2021.

[5] M. Haghani, F. Sprei, K. Kazemzadeh, Z. Shahhoseini, and J. Aghaei, "Trends in electric vehicles research," *Transportation Research Part D: Transport and Environment*, vol. 123, article 103881, 2023.

[6] V. Bolborici, F. P. Dawson, and K. K. Lian, "Hybrid energy storage systems: connecting batteries in parallel with ultracapacitors for higher power density," *IEEE Industry Applications Magazine*, vol. 20, no. 4, pp. 31–40, 2014.

[7] A. Katnapally, U. B. Manthati, A. Chirayarukil Raveendran, and S. Punna, "A predictive power management scheme for hybrid energy storage system in electric vehicle," *International*

Journal of Circuit Theory and Applications, vol. 49, no. 11, pp. 3864–3878, 2021.

[8] A. S. Mohammed, S. M. Atnaw, A. O. Salau, and J. N. Eneh, "Review of optimal sizing and power management strategies for fuel cell/battery/super capacitor hybrid electric vehicles," *Energy Reports*, vol. 9, pp. 2213–2228, 2023.

[9] S. Koohi-Fayegh and M. A. Rosen, "A review of energy storage types, applications and recent developments," *Journal of Energy Storage*, vol. 27, article 101047, 2020.

[10] I. Azizi and H. Radjeai, "A new strategy for battery and supercapacitor energy management for an urban electric vehicle," *Electrical Engineering*, vol. 100, no. 2, pp. 667–676, 2018.

[11] E. D. Kostopoulos, G. C. Spyropoulos, and J. K. Kaldellis, "Real-world study for the optimal charging of electric vehicles," *Energy Reports*, vol. 6, pp. 418–426, 2020.

[12] F. Nadeem, S. M. S. Hussain, P. K. Tiwari, A. K. Goswami, and T. S. Ustun, "Comparative review of energy storage systems, their roles, and impacts on future power systems," *IEEE Access*, vol. 7, pp. 4555–4585, 2019.

[13] A. Aswakumar Geetha, A. Bernonse Vasantha, H. K. Raveendran Pillai, and U. Somarajan, "Battery and supercapacitor assisted controller for stability enhancement of DC microgrid," *International Journal of Circuit Theory and Applications*, vol. 50, no. 12, pp. 4357–4375, 2022.

[14] E. Chemali, M. Preindl, P. Malysz, and A. Emadi, "Electrochemical and electrostatic energy storage and management systems for electric drive vehicles: state-of-the-art review and future trends," *IEEE Journal of Emerging and Selected Topics in Power Electronics*, vol. 4, no. 3, pp. 1117–1134, 2016.

[15] S. Elouarouar, H. Medromi, and F. Moutaouakkil, "Energy Management in Multi-Rotors Unmanned Aerial Systems," in *2017 International Renewable and Sustainable Energy Conference (IRSEC)*, pp. 1–7, Tangier, Morocco, 2017.

[16] A. Khaligh and Z. Li, "Battery, ultracapacitor, fuel cell, and hybrid energy storage systems for electric, hybrid electric, fuel cell, and plug-in hybrid electric vehicles: state of the art," *IEEE Transactions on Vehicular Technology*, vol. 59, no. 6, pp. 2806–2814, 2010.

[17] T. S. Babu, K. R. Vasudevan, V. K. Ramachandaramurthy, S. B. Sani, S. Chemud, and R. M. Lajim, "A comprehensive review of hybrid energy storage systems: converter topologies, control strategies and future prospects," *IEEE Access*, vol. 8, pp. 148702–148721, 2020.

[18] S. Punna, U. B. Manthati, and A. Chirayarukil Raveendran, "Modeling, analysis, and design of novel control scheme fortwo-inputbidirectionalDC-DCconverter forHESSinDCmicrogrid applications," *International Transactions on Electrical Energy Systems*, vol. 31, no. 10, article e12774, 2021.

[19] R. Bhosale and V. Agarwal, "Fuzzy logic control of the ultracapacitor interface for enhanced transient response and voltage stability of a DC microgrid," *IEEE Transactions on Industry Applications*, vol. 55, no. 1, pp. 712–720, 2019.

[20] S. Chen, Q. Yang, J. Zhou, and X. Chen, "A model predictive control method for hybrid energy storage systems," *CSEE Journal of Power and Energy Systems*, vol. 7, no. 2, pp. 329–338, 2020.

[21] D. B. W. Abeywardana, B. Hredzak, and V. G. Agelidis, "A fixed-frequency sliding mode controller for a boost-inverter-based battery-supercapacitor hybrid energy storage system," *IEEE Transactions on Power Electronics*, vol. 32, no. 1, pp. 668–680, 2017.

[22] P. Singh and J. S. Lather, "Dynamic current sharing, voltage and SOC regulation for HESS based DC microgrid using CPISMC technique," *Journal of Energy Storage*, vol. 30, article 101509, 2020.

[23] P. Victor, *Electrotechnical Systems Simulation with Simulink and Simpowersystems*, CRC Press, Boca Raton, 2013.

[24] C. R. Arunkumar, U. B. Manthati, and S. Punna, "Supercapacitor voltage based power sharing and energy management strategy for hybrid energy storage system," *Journal of Energy Storage*, vol. 50, article 104232, 2022.

[25] S. Punna, U. B. Manthati, and C. R. Arunkumar, "A comparative analysis of PI and predictive control strategy for HESS based bi-directional DC-DC converter for DC microgrid applications," in *Next Generation Smart Grids: Modeling, Control and Optimization*, pp. 181–220, Springer Nature Singapore, Singapore, 2022.

[26] M. C. Joshi and S. Samanta, "Improved energy management algorithm with time-share-based ultracapacitor charging/discharging for hybrid energy storage system," *IEEE Transactions on Industrial Electronics*, vol. 66, no. 8, pp. 6032–6043, 2019.

[27] A. Mehta and B. Naik, *Sliding Mode Controllers for Power Electronic Converters*, Springer, Singapore, 2019.

[28] F. Yusivar, N. Hidayat, R. Gunawan, and A. Halim, "Implementation of field oriented control for permanent magnet synchronous motor," in *2014 International Conference on Electrical Engineering and Computer Science (ICEECS)*, pp. 359–362, Kuta, Bali, Indonesia, 2014.